

Wide-band quantum interface for visible-to-telecommunication wavelength conversion

Rikizo Ikuta,¹ Yoshiaki Kusaka,¹ Tsuyoshi Kitano,¹ Hiroshi Kato,¹
Takashi Yamamoto,¹ Masato Koashi,² and Nobuyuki Imoto¹

¹*Graduate School of Engineering Science, Osaka University,
1-3 Machikaneyama, Toyonaka, Osaka 560-8531, Japan*

²*Photon Science Center, The University of Tokyo,
2-11-16 Yayoi, Bunkyo-ku, Tokyo 113-8656, Japan*

We perform the first demonstration of a quantum interface for frequency down-conversion from visible to telecommunication bands by using a nonlinear crystal. This interface has a potential to work over wide bandwidths, leading to a high-speed interface of frequency conversion. We achieve the conversion of a pico-second visible photon at 780 nm to a 1522-nm photon, and observe that the conversion process retain entanglement between the down-converted photon and another photon.

Photons play an important role for transmitting a quantum state among distantly located physical systems, such as atoms, ions, and solid-state systems [1–5], which are used as memories and/or processors of quantum communication [6, 7] and information processing[8]. So far, experimental demonstrations aiming at such tasks have been actively done with photons in visible wavelengths [9, 10]. However, when we look at long-distance quantum communication [11], a near-infrared wavelength within telecommunication bands is vital for efficient optical fiber communications. This optical frequency mismatch can be filled by frequency conversion of a photon while preserving its quantum state [12]. A pioneer work of such a quantum interface for the optical frequency conversion has been done by using a second-order nonlinearity in a periodically-poled LiNbO₃ (PPLN) crystal [13], in which a photon of a telecom wavelength was up-converted to a visible one. Such a frequency up-conversion was also actively studied for efficient detection of photons in telecommunication bands [14]. On the other hand, quantum interfaces for frequency down-conversion from visible to telecommunication bands have recently been demonstrated by using a third-order nonlinearity of a dense atomic cloud [15, 16], which uses two pump lights MHz-detuned from resonant frequencies of the atom. In these demonstrations, choice of the target wavelength is severely limited to the vicinity of the resonant frequency of the atom. Such a restriction on frequency selections can be relaxed by using a bulk nonlinear crystal. So far, aiming at such a versatile quantum interface, demonstrations of difference-frequency generation (DFG) in nonlinear optical crystals with a strong pump and a weak coherent light seed have been performed [17, 18].

In this Letter, we present the first demonstration of DFG-based frequency down-conversion of non-classical light by a nonlinear optical crystal from a visible wavelength at 780 nm to a telecommunication wavelength at 1522 nm. Using a waveguided PPLN crystal with a wide acceptable bandwidth as the second-order nonlinear optical material, we have observed sub-Poissonian

photon statistics of the light at 1522 nm after the frequency down-conversion of a pico-second single-photon pulse at 780 nm. Then, we have demonstrated the frequency down-conversion of one half of a 780-nm entangled photon pair, and observed the entanglement between the down-converted photon at 1522 nm and the other half at 780 nm.

The quantum theory of frequency conversion of single-mode pulsed light using a second-order nonlinear optical interaction is as follows. When the pump light at angular frequency ω_p is sufficiently strong, the quantum dynamics of a signal mode at angular frequency ω_s and a converted mode at angular frequency ω_c satisfying $\omega_c = \omega_s - \omega_p$ is described by the following Hamiltonian:

$$\hat{H} = i\hbar(\xi^* \hat{a}_c^\dagger \hat{a}_s - \xi \hat{a}_s^\dagger \hat{a}_c), \quad (1)$$

where \hat{a}_s and \hat{a}_c are annihilation operators of the signal mode and the converted mode, respectively. A coupling constant $\xi = |\xi|e^{i\phi}$ of the nonlinear optical medium is proportional to the complex amplitude of the classical pump light, where ϕ is the phase of the pump light. Using the Heisenberg representation $\hat{a}_{s(c)}(t) \equiv \hat{U}^\dagger \hat{a}_{s(c)} \hat{U}$ with $\hat{U} \equiv \exp(-i\hat{H}t/\hbar)$, annihilation operators $\hat{a}_{s,\text{out}}$ and $\hat{a}_{c,\text{out}}$ of the signal and converted modes coming out from the nonlinear medium are written as

$$\hat{a}_{s,\text{out}} = \hat{a}_s(\tau) = \cos(|\xi|\tau) \hat{a}_s - e^{i\phi} \sin(|\xi|\tau) \hat{a}_c \quad (2)$$

and

$$\hat{a}_{c,\text{out}} = \hat{a}_c(\tau) = e^{-i\phi} \sin(|\xi|\tau) \hat{a}_s + \cos(|\xi|\tau) \hat{a}_c, \quad (3)$$

where τ is the traveling time of the pulses through the nonlinear medium. The process of the frequency conversion described in equations (2) and (3) can be regarded as a beamsplitter in the frequency degree of freedom with the transmittance of $\cos^2(|\xi|\tau)$. A condition $|\xi|\tau = \pi/2$ for the complete conversion is achieved by adjusting the amplitude of the pump light and the length of the nonlinear medium.

As a preliminary experiment, we performed the frequency down-conversion of a classical light in a coherent

state. Our experimental setup is shown in Fig. 1 (a). We use a mode-locked Ti:sapphire (Ti:S) laser as a signal light source. The center wavelength is 780 nm, the pulse width is 1.2 ps, and the repetition rate is 82 MHz. After passing through a polarization-maintaining fiber (PMF), the signal beam is set to vertical (V) polarization by a polarization beamsplitter (PBS) and a half-wave plate (HWP). The signal beam is diffracted by a Bragg grating (BG1) which narrows the bandwidth to 0.2 nm. A seed laser beam from an external cavity diode laser (ECDL) at 1600 nm with a linewidth of $\Delta f \equiv 150$ kHz is amplified by an Erbium-doped fiber amplifier (EDFA), and then it is used as a pump light for the DFG. We use BG2 with the bandwidth of 1 nm for suppressing unnecessary frequency components of the pump light. The power of the pump light is adjusted by a variable attenuator (VA) composed of a HWP and a PBS. The signal and pump lights are set to V polarization and combined at a dichroic mirror (DM), and then focused on the PPLN crystal.

The PPLN waveguide in our experiments consists of Zn-doped lithium niobate as the waveguide core and lithium tantalite as the cladding layer [19]. The waveguide is a ridged type with 8- μm wide, and its length is 20 mm. The periodically-poled structure has an 18- μm period designed for the type-0 quasi-phase matching. The best conversion efficiency was obtained at the temperature of 50°C. The acceptable phase-matching bandwidth for the 780-nm signal light of the 20-mm long crystal is calculated to be about 0.3 nm.

After passing through the PPLN waveguide, the strong pump light is diminished by a high-pass filter (HPF) and the converted light at 1522 nm is extracted by BG3 with a bandwidth of 1 nm. Finally the beam is coupled into a single-mode fiber by a fiber coupler (FC1) and connected to a power meter. The photon conversion efficiency of the PPLN was observed as shown in Fig. 1 (b). The maximum conversion efficiency was ≈ 0.62 at 700-mW pump power coupled to the PPLN waveguide. The transmittance of the optical components from the end of the PPLN to the power meter was estimated to be ≈ 0.62 . This gives the overall conversion efficiency from the 780-nm photon coupled in the PPLN to the 1522-nm photon coupled to the fiber as ≈ 0.39 . The conversion efficiency will be improved when the linewidth of the signal light becomes much narrower than the acceptable linewidth of the PPLN waveguide. When we used a 780-nm cw light from an ECDL with a 3-MHz linewidth, we observed the maximum conversion efficiency of 0.71.

The preservation of the photon statistics of the signal light after the frequency conversion is the first step toward the demonstration of our quantum interface. Non-classical behavior of the photon statistics of the pulsed light appears in the second-order intensity correlation

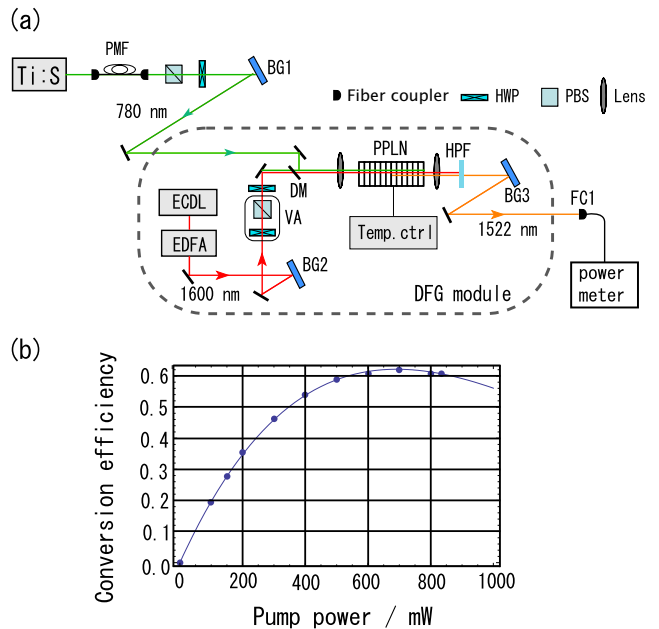


FIG. 1: Frequency down-conversion of coherent light pulse. (a) Experimental setup. The signal light from the mode-locked Ti:sapphire (Ti:S) laser at 780 nm and the pump beam from the external cavity diode laser (ECDL) at 1600 nm are combined at the dichroic mirror (DM). Then, they are coupled into the PPLN for the frequency down-conversion to the 1522-nm wavelength. The light at 1522 nm is extracted using the high-pass filter (HPF) and the Bragg grating (BG3) with a 1-nm bandwidth, and coupled to the single-mode fiber. (b) The conversion efficiency depending on the power of the pump light coupled to the PPLN. The maximum conversion efficiency ≈ 0.62 was obtained at 700-mW pump power. A solid curve is fitted using a function $A \sin^2(\sqrt{BP_{\text{pump}}})$ expected from equation (2), where P_{pump} is the pump power. Parameters A and B are estimated as 0.62 and 3.6 (mW) $^{-1}$, respectively.

function between the n th neighbor pulses defined by

$$g_n^{(2)} \equiv \frac{\left\langle : \int \hat{I}(t) dt \int \hat{I}(t+nT) dt : \right\rangle}{\left\langle \int \hat{I}(t) dt \right\rangle \left\langle \int \hat{I}(t+nT) dt \right\rangle}, \quad (4)$$

where $\hat{I}(t)$ is an intensity operator at time t , T is the time interval of the pulses, and the integrations are over a range of the single-pulse duration. The product of the operators is in normal order and time order [20]. While $g_0^{(2)} \geq 1$ is always satisfied in the classical wave theory, the quantization of light allows the possibility that $g_0^{(2)}$ is smaller than 1, with the smallest value $g_0^{(2)} = 0$ for an ideal single-photon pulse. The experimental setup for frequency down-conversion of a single photon at 780 nm followed by correlation measurement on the converted light is shown in Fig. 2. A photon pair A and B are generated by spontaneous parametric down-conversion (SPDC) at

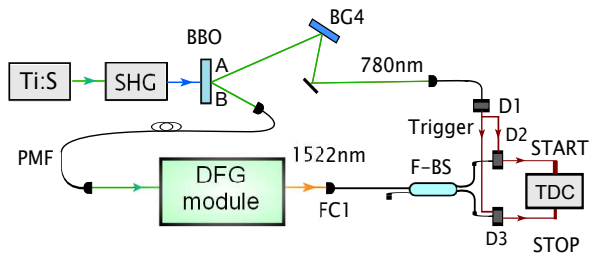


FIG. 2: Frequency down-conversion of heralded single photons at 780 nm. The light pulse from the Ti:S laser is frequency doubled to the wavelength of 390 nm by second harmonic generation (SHG), and then pumps a Type-I phase-matched 1.5mm-thick BBO crystal to prepare a photon pair A and B at 780 nm by spontaneous parametric down-conversion. The photon in mode A is detected by a silicon avalanche photodiode detector D1 connected to a single-mode fiber for the preparation of the heralded single photon in mode B. We observe the second-order intensity correlation function $g_0^{(2)}$ of the light converted to 1522 nm using the Hanbury-Brown and Twiss setup.

a β -barium borate (BBO) crystal, and the presence of a single photon in mode B is heralded by detection of a photon in mode A by a photon detector D1. The spectral filtering of the photon in mode A is performed by BG4 with a bandwidth of 0.2 nm. The wavelength of the heralded single photon is converted to 1522 nm by the DFG module described in Fig. 1 (a). The converted pulse is coupled to FC1, and its second-order intensity correlation $g_0^{(2)}$ is measured by using a Hanbury-Brown and Twiss setup [21, 22], which consists of a fiber-optic beamsplitter (F-B) and photon detectors D2 and D3. D2 and D3 are InGaAs/InP avalanche photodiodes gated by trigger signals from D1. To measure the temporal difference between the detections at D2 and D3 with high resolution, signals from D2 and D3 are input to a time-to-digital converter (TDC) as a start and a stop signal of the clock, respectively. By recording the trigger counts N_{trig} from D1, the start counts N_{start} from D2, the stop counts N_{stop} from D3, and coincidence counts N_{coinc} within 1 ns from the TDC, we determine $g_0^{(2)}$ by

$$g_0^{(2)} = \frac{N_{\text{trig}} N_{\text{coinc}}}{N_{\text{start}} N_{\text{stop}}}. \quad (5)$$

The measured $g_0^{(2)}$ of the light converted from the heralded single photon at 780 nm was 0.17 ± 0.04 , which is much smaller than one, and indicates sub-Poissonian photon statistics of the converted light. This result clearly shows that the non-classical property of the light survived after the frequency down-conversion. The nonzero value of $g_0^{(2)}$ is mainly caused by optical noises from the PPLN. They are linearly increasing with the pump power when the signal light is turned off, which may suggest that they are caused by Raman scatter-

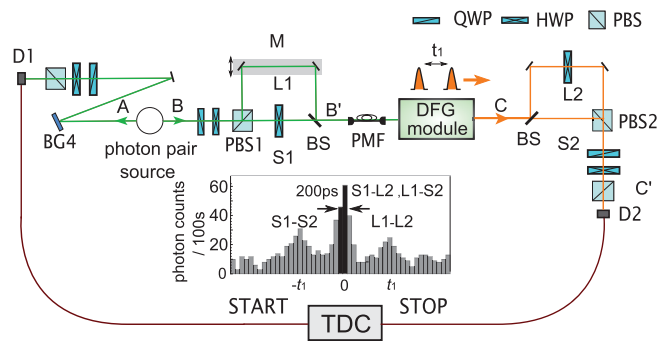


FIG. 3: Frequency down-conversion of one halves of polarization-entangled photon pairs. At the photon pair source, the light pulse from the Ti:S laser is frequency doubled by SHG, and pumps a pair of BBO crystals to prepare the entangled photon pair $|\phi^+\rangle_{AB}$ through SPDC [24]. The frequency down-conversion of photon B is performed after encoding a polarization qubit into a time-bin qubit using an unbalanced MZI, then decoding it back to the polarization qubit after frequency down-conversion. The histogram shows the number of coincidence events with various delay between the detectors D1 and D2, which were recorded by the TDC. The measurement bases of photons in modes A and C' are set as $+45^\circ$ polarization. The central peak shows the events where the photon has passed through S1-L2 or L1-S2, and the two peaks separated from the central peak by t_1 correspond to the cases where the photon has passed through S1-S2 or L1-L2. We accept the events in 200-ps time window around the central peak as the successful events.

ing [23].

Finally, we performed the frequency down-conversion of one halves of polarization-entangled photon pairs at 780 nm. The experimental setup is shown in Fig. 3. A photon pair source prepares a polarization-entangled photon pair A and B described as $|\phi^+\rangle_{AB} \equiv (|HH\rangle_{AB} + |VV\rangle_{AB})/\sqrt{2}$. The spectral filtering of photon A is performed by BG4. Photon B goes to an unbalanced Mach-Zehnder interferometer (MZI). At the MZI, PBS1 separates H and V polarization into a short path (S1) and a long path (L1), respectively. After horizontal (H) polarization is flipped to V polarization by a HWP inserted into S1, modes S1 and L1 are mixed by a BS. This transforms the polarization qubit in mode B to a time-bin qubit in mode B', and the initial two-photon state $|\phi^+\rangle_{AB}$ becomes a polarization and time-bin entangled state

$$|\psi\rangle_{AB'} \equiv \frac{1}{\sqrt{2}}(|H\rangle_A |S1\rangle_{B'} + |V\rangle_A |L1\rangle_{B'}), \quad (6)$$

where $|S1\rangle$ and $|L1\rangle$ represent the states of the V-polarized photons passing through S1 and L1, respectively. After passing through a PMF, the photon in mode B' goes to the DFG module.

The light down-converted by the DFG process inherits the phase $-\phi$ of the pump light as described in equation (2). Then, through the frequency down-conversion,

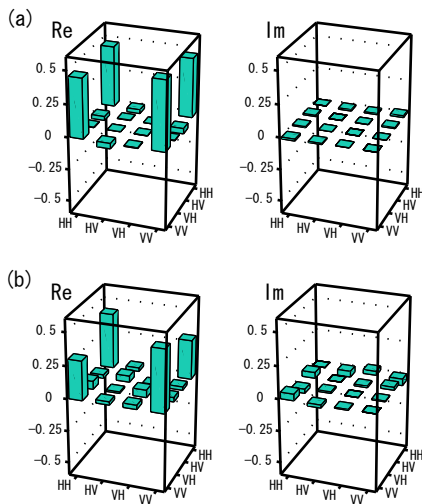


FIG. 4: The reconstructed density matrices. (a) The initial entangled photon pair ρ_{AB} prepared by the photon pair source. (b) The two-photon state $\rho_{AC'}$ between the 780-nm photon in mode A and the 1522-nm photon in mode C' . The overall detection rate of each photon pair ρ_{AB} and $\rho_{AC'}$ is 492 Hz and 2.4 Hz, respectively.

the former and the latter term in equation (6) receive phase shifts $-\phi(t)$ and $-\phi(t + t_1)$ from the pump light, respectively. In our experiment, since t_1 is about 1 ns and Δf is 150 kHz, the coherence time $1/(2\pi\Delta f) \approx 1\mu\text{s}$ of the pump light is much longer than t_1 , which ensures that $\phi(t) = \phi(t + t_1)$ is satisfied. As a result, we should obtain the state $|\psi\rangle_{AC}$ for the 780-nm photon and the 1522-nm photon in mode C.

The down-converted photon in mode C is fed to the second unbalanced MZI. A BS in the MZI divides the converted photon into a short path (S2) and a long path (L2). A HWP inserted in L2 flips the polarization from V to H. Two modes S2 and L2 are recombined by PBS2. This transforms the degree of freedom from time-bin to polarization. After the MZI, the photon in mode C' goes to detector D2 which is gated by trigger counts from D1. The path lengths S1-L2 and L1-S2 are adjusted by the mirrors M on a motorized and piezo-driven stage. When we post-select the events where the photon has passed through S1-L2 or L1-S2, we should obtain the polarization-entangled state $|\phi^+\rangle_{AC'}$ for the two photons in modes A and C' . In our experiment, we accept such events in 200-ps time window shown in the histogram in the inset of Fig. 3.

We first performed quantum state tomography of 780-nm photon pairs in modes A and B from the photon pair source. The required polarization correlations have been measured by rotating a quarter-wave plate (QWP) and a HWP in mode A, and a QWP and a HWP before PBS1 in mode B [25]. The PMF before the DFG module was connected to a silicon avalanche photodiode. The ob-

served density operator ρ_{AB} of the two-photon state is shown in Fig. 4 (a). The iterative maximum likelihood method was used for the reconstruction of ρ_{AB} [26, 27]. The observed fidelity of ρ_{AB} to $|\phi^+\rangle_{AB}$ was 0.95 ± 0.01 , which implies that the photon pair source prepared a highly entangled 780-nm photon pair. Next, we performed quantum state tomography between the photon in mode A and the converted photon in mode C' . The reconstructed density operator $\rho_{AC'}$ of the state is shown in Fig. 4 (b). We calculated the fidelity and entanglement of formation [28] from reconstructed $\rho_{AC'}$ as 0.75 ± 0.06 and 0.36 ± 0.13 , respectively. The observed value of the fidelity is greater than $1/\sqrt{2} \approx 0.707$, which implies that the entangled state $\rho_{AC'}$ can violate the Clauser-Horne-Shimony-Holt (CHSH) inequality. We note that when we subtract background noises whose rate is about 0.2 Hz in each basis from the observed coincidence counts, the fidelity of the output state becomes 0.95, which shows that the degradation is mainly caused by the optical noises from the PPLN.

In conclusion, we have demonstrated frequency down-conversion of non-classical light at 780 nm to a telecommunication wavelength of 1522 nm by using the DFG process in the PPLN waveguide. Our quantum interface has down-converted the frequency of one half of the visible entangled photon pair to the telecommunication wavelength while preserving entanglement. The DFG process with the quasi-phase-matching techniques allows us to convert a wide range of visible wavelengths to telecommunication ones with a wide acceptable bandwidth. We believe such a quantum interface will be useful for long distance quantum communication based on various visible photon emitters including atomic quantum memories.

We thank Toshiyuki Tashima and Hirokazu Kobayashi for helpful discussions. This work was supported by the Funding Program for World-Leading Innovative R & D on Science and Technology (FIRST), MEXT Grant-in-Aid for Scientific Research on Innovative Areas 20104003 and 21102008, MEXT Grant-in-Aid for Young scientists(A) 23684035, and the MEXT Global COE Program.

-
- [1] D. N. Matsukevich and A. Kuzmich, *Science* **306**, 663 (2004).
 - [2] W. Rosenfeld *et al.*, *Phys. Rev. Lett.* **101**, 260403 (2008).
 - [3] S. Olmschenk *et al.*, *Science* **323**, 486 (2009).
 - [4] E. Togan *et al.*, *Nature* **466**, 730 (2010).
 - [5] T. Müller *et al.* *cond-mat/arXiv:1101.4911* (2011).
 - [6] H. -J. Briegel *et al.*, *Phys. Rev. Lett.* **81**, 5932 (1998).
 - [7] L. M. Duan *et al.*, *Nature (London)* **414**, 413 (2001).
 - [8] J. I. Cirac and P. Zoller, *Nature (London)* **404**, 579 (2000).
 - [9] Z. Zhao *et al.*, *Phys. Rev. Lett.* **90**, 207901 (2003).
 - [10] P. Walther *et al.*, *Nature (London)* **434**, 169 (2005).
 - [11] N. Gisin and R. Thew, *Nature Photonics* **1**, 165 (2007).
 - [12] P. Kumar, *Opt. Lett.* **15**, 1476 (1990).

- [13] S. Tanzilli *et al.*, Nature (London) **437**, 116 (2005).
- [14] C. Langrock, *et al.*, Opt. Lett. **30**, 1725 (2005).
- [15] A. G. Radnaev *et al.*, Nature Physics **6**, 894 (2010).
- [16] Y. O. Dudin *et al.*, Phys. Rev. Lett. **105**, 260502 (2010).
- [17] H. Takesue, Phys. Rev. A **82**, 013833 (2010).
- [18] N. Curtz *et al.*, Opt. Express **18**, 22099 (2010).
- [19] T. Nishikawa *et al.*, Opt. Express **17**, 17792 (2009).
- [20] M. Koashi *et al.*, Phys. Rev. Lett. **71**, 1164 (1993).
- [21] R. H. Brown and R. Q. Twiss, Nature **178**, 481 (1956).
- [22] M. Beck, J. Opt. Soc. Am. B. **24**, 2972 (2007).
- [23] N. A. Peters *et al.*, New J. Phys. **11**, 045012 (2009).
- [24] T. Yamamoto *et al.*, Nature Photonics **2**, 488 (2008).
- [25] D. F. V. James *et al.*, Measurement of qubits. Phys. Rev. A **64**, 052312 (2001).
- [26] J. Řeháček, and Z. Hradil, Phys. Rev. A **75**, 042108 (2007).
- [27] T. Tashima *et al.*, Phys. Rev. Lett. **102**, 130502 (2009).
- [28] W. K. Wootters, Phys. Rev. Lett. **80**, 2245 (1998).